GPNLPerf: Robust 4d Non-rigid Motion Correction for Myocardial Perfusion Analysis

S. Thiruvenkadam[1(✉)], K. S. Shriram[1], B. Patil[1], G. Nicolas[2], M. Teisseire[2], C. Cardon[2], J. Knoplioch[2], N. Subramanian[1], S. Kaushik[1], and R. Mullick[1]

[1] GE Global Research, Bangalore, India
sheshadri.thiruvenkadam@ge.com
[2] GE Healthcare, Buc, France

Abstract. Since the introduction of wide cone detector systems, CT myocardial perfusion has been an area of increased interest, for which non-rigid registration [NRR] is a key step to further analysis. We propose a novel motion management pipeline for perfusion data, GPNLPerf (*Group-wise, non-local, NRR for perfusion analysis*) centering on group-wise NRR using non-local spatio-temporal constraints. The proposed pipeline deals with the NRR challenges for 4D perfusion data and results in generating clinically relevant perfusion parameters. We demonstrate results on 9 dynamic perfusion exams comparing results quantitatively with ANTs NRR and also show qualitative results on perfusion maps.

1 Introduction

Full coverage dynamic CT contrast scans are key to quantify myocardial perfusion parameters such as blood flow which are key to the diagnosis of cardiac disease [1]. An important challenge that needs to be addressed for computing reliable perfusion maps is motion induced by repiration and cardiac movement. Such respiratory/cardiac motion would result in gross errors in the estimated perfusion maps. In this work, we propose a fully automatic end-end solution for addressing the motion challenges of 4D CT perfusion studies. In order to deduce clinically meaningful perfusion parameters, any NRR approach has to handle challenges of large motion, intensity variations due to contrast dynamics, and presence of small structures like vessels. Further, it is important for NRR to preserve the inherent contrast dynamics, and work in a feasible compute time. Although there have been several works for NRR of perfusion data in the context of dynamic CT perfusion ([2,3]) and for DCE MR ([4,5]), previous works have not fully handled the above challenges to offer a viable clinical solution.

Two broad categories of aligning 4D data are '*reference*' based methods and *groupwise* NRR (see [6]). Unlike reference based methods, groupwise NRR is not biased by the choice of the reference image. In general, for cardiac contrast data, there are dramatic changes in intensity that vary spatially, with structures becoming visible at different time points. Thus, large differences in NRR results could occur depending on the choice of the reference image. Hence, groupwise NRR could prove quite useful for dynamic cardiac perfusion data.

S. Ourselin et al. (Eds.): MICCAI 2016, Part III, LNCS 9902, pp. 255–263, 2016.
DOI: 10.1007/978-3-319-46726-9_30

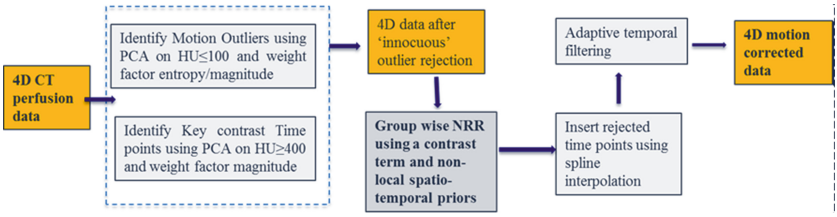

Fig. 1. GPNLPerf: pipeline composed of (a) Outlier Rejection and interpolation (b) Group-wise NRR (c) Adaptive temporal filtering.

However, a challenge for groupwise NRR is to handle small populations of data with large motion in the absence of a good initial guess for both the evolving reference image and the transforms. Previous groupwise NRR methods for perfusion data, [4,5], have been for 2D DCE MRI data where typically several timepoints [TPs] are available giving a good initial guess for the groupwise mean. Secondly, schemes such as breaking the data into groups of pre- and post-contrast as in [4] may not be feasible for CT cardiac perfusion given that there might be very few TPs (e.g. 12–15) with large regions peaking with contrast at different times. In [7], the issue of large motion for small populations within groupwise NRR is handled for PET data using non-local spatio-temporal penalties. In our work, we address groupwise NRR for CT dynamic perfusion data, adapting and extending the framework in [7]. As a result, compared to previous groupwise NRR works for perfusion, we can effectively handle the challenge of large motion of small number of TPs.

Our proposed solution GPNLPerf is a generic pipeline composed of (a) Outlier Rejection and interpolation (b) Robust group-wise NRR using non-local spatio-temporal constraints, and (c) Adaptive temporal filtering. Firstly, we call out 'innocuous' TPs with extreme motion as outliers and drop them from 4D NRR. These TPs are later interpolated from neighbouring registered TPs. Next, in the core of the algorithm, we propose a metric that models the contrast dynamics seen in perfusion studies, within the groupwise NRR approach [7]. Lastly, to meet computational feasibility for clinically deployment, we run NRR at a manageable lower resolution and later arrest the jitter due to interpolation effects using an adaptive temporal filtering approach. Results are analyzed on 9 dynamic perfusion exams. We quantitatively compare our performance to a pairwise approach using the ANTs package. Finally, a qualitative assessment of reconstructed perfusion maps is presented using standard visualization.

2 Methods

Here, we describe the proposed GPNLPerf pipeline. Firstly, we drop out TPs with extreme motion especially if they would play no role in the final perfusion map computation. Typically, in breathhold acquisitions, when the patient starts to free breathe, there is extreme motion in 1 or 2 transition TPs. If these extreme

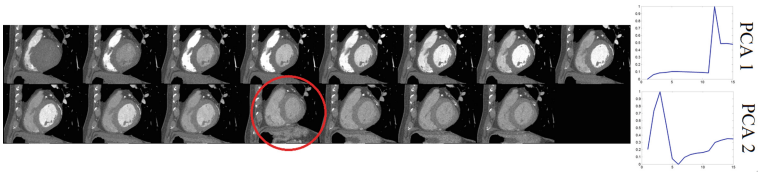

Fig. 2. Outlier Rejection for a 4D CT case with 15 TPs: An 'innocuous' outlier timepoint (highlighted in Red) is rejected because the resulting PCA weight factors are large (first plot). The timepoint is innocuous since it does not have peak contrast activity and this is seen in the weight factors of the 2nd PCA step (second plot).

TPs lie in 'innocuous' locations from a contrast dynamics point of view, these volumes can be safely dropped without the risk of altering the end perfusion maps. After NRR, these rejected temporal positions can be re-inserted using interpolation. The algorithm flow is shown in Fig. 1.

2.1 PCA Based Outlier Rejection

The objective here is to conservatively reject one or two time points as motion outliers and also make sure that they are not key time points for the contrast dynamics. Here, we use a simple two stage technique based on Principal Component Analysis (PCA) to achieve the above. Firstly, motion outliers are identified by limiting the dynamic range of the data to air and soft tissue, Hounsfield Unit HU ≤ 200. This data, after spatial down sampling is passed through PCA to get the principal eigenvectors (restricted to the first two) that quantify large motion directions. Projecting the eigen vectors back to the data gives the weight factors that quantifies the motion of each timepoint in the direction of the eigenvectors. Motion outliers (not more than two TPs) if any, are then identified by looking at entropy and magnitude of these temporal weight factors. Entropy is a key feature here to distinguish cases with large motion in several time points (e.g. data from a free breathing protocol), for which an outlier rejection step would not make sense. Next, to make sure that only 'innocuous' time points are rejected, we perform one more round of PCA in a higher range HU ≥ 400, to consider only contrast induced intensity changes across time points. Now, large weight factors corresponding to first two eigen vectors would tell us the interesting TPs from a contrast dynamics perspective. If the motion outliers do not fall in the set of interesting TPs, we can safely reject them as 'innocuous' TPs (example of utility of the two PCA steps are shown in Fig. 2). Post NRR, these rejected TPs are inserted using standard spline interpolation using neighboring TPs.

2.2 Non-local Group-Wise NRR for Perfusion Data

In this discussion, we address the main contribution of the paper; NRR of the outlier rejected data. We propose a group-wise NRR energy in a variational framework with non-local spatio temporal penalties on the transforms. We adapt

the mono-modal groupwise formulation from [7] proposed for gated PET data, to handle intensity variations seen in CT perfusion. To do this, we add an additional contrast term to distinguish intensity changes due to motion from intensity changes due to contrast flow. Assume we are given N volumes $\{I_k^o\}_{k=1}^N$ defined on Ω. Firstly, the input volumes are preprocessed to lie in the HU range [−200,400] where we would see minimal contrast dynamics, to give N preprocessed volumes $\{J_k\}_{k=1}^N$. We seek a reference volume μ_{med} and deformation fields $\{w_k\}_{k=1}^N$, $\mathbf{w} = [w_1, w_2, ..., w_N]$, which minimizes:

$$L[\mu_{med}, \mathbf{w}] = \sum_{k=1}^{N} \int_{\Omega} |J_k(. + w_k) - \mu_{med}| dx + \alpha \int_{\Omega} |(Id - VV^T)(I_{\mathbf{w}}^o - \mu_{I_o})|^2 dx$$
$$+ \beta \sum_{k=1}^{N} \int_{\Omega} \int_{\Omega} m(x,y) |w_k(x) - w_k(y)|^2 dxdy$$
$$+ \beta_1 \sum_{k=1}^{N} \int_{\Omega} \int_{\Omega} \hat{m}(x,y) |v_k(x) - v_k(y)|^2 dxdy$$

This is a groupwise formulation with the data term tuned to handle contrast dynamics. The first term minimizes the voxel wise median deviation of the 4D data. The above term can be minimized by iteratively solving for the median of the data, μ_{med}, and the transforms $\mathbf{w}$. The second term seeks transforms so that the registered 4D data (i.e. the transforms $\mathbf{w}$ applied to the original data I^o) conforms to learnt contrast trends. Here, we utilize a contrast model term which uses contrast trends learnt from coarse resolutions. We use PCA once again to learn principal directions of variation in contrast, V and mean trend, μ_{I_o}. The contrast term is useful in finer resolutions to align smaller structures better and reduce artefacts due to intensity variations induced by contrast dynamics.

Similar to [7], the regularization terms on the transforms $\mathbf{w}$ consist of a non-local [NL] spatial term, and a NL temporal term seeking spatial coherence of velocity $v_k = w_{k+1} - w_k$. The NL penalties are critical in robustly handling large motion, residual intensity variations (inspite of pre-processing and the contrast term), and maintaining integrity of key structures such as myocardium and coronories. Scalars α, β, β_1 balance the terms; $m(x,y)$, $\hat{m}(x,y)$ are spatial weight functions defined by Gaussians. We minimize the above equation using steepest descent, in a multi-resolution framework. In the coarse resolutions, the contrast term is turned off, i.e. $\alpha = 0$. The contrast trends V, μ_{I_o} learnt at the end of coarse resolutions are then applied in finer resolutions. A brief illustration and importance of contributions of the NL terms and the contrast term is shown in a synthetic experiment, Fig. 3. As seen, the contrast term handles NRR better under contrast dynamics (thus distinguishing our work from [7] which is susceptible to intensity variations, third row, Fig. 3.

2.3 Adaptive Temporal Filtering

Lastly, given that we want a computationally tractable solution, the deformation fields are at a finest resolution of 1.5 mm^3 while the original data is typically

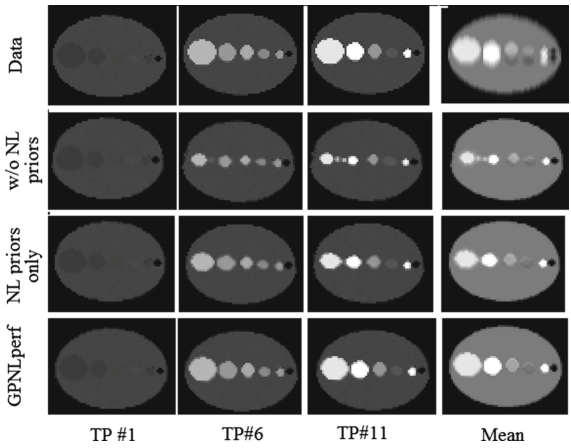

Fig. 3. Contribution of the NL priors and the contrast term: the synthetic data (first row) has 11 TPs, results for 3 TPs are shown in columns 1 to 3. The last column is the mean across TPs. The second row is Eq. 1 w/o any priors. The contrast dynamics combined with motion creates artefacts (e.g. shrinking of bright structures) in the registered images. The third row shows slightly improved results with only the NL priors (as in [7]). The last row shows the best results with the contrast term and the NL priors (GPNLPerf).

at higher resolution. For visualizing the perfusion maps and the registered data, the deformation fields are upsampled and applied to the original data at native resolution. The resulting jitter artifacts due to this interpolation step is handled using a simple temporal filtering step. A moving temporal median filter is employed at each voxel location. The median filter is also made adaptive to work only in non-contrast regions (defined using a smooth sigmoid cutoff on a suitable HU range ≤ 400).The above adaptive filter ensures that interpolation artifacts are arrested and contrast activity is preserved for the perfusion maps.

3 Experiments

We show a qualitative example in Fig. 4 with large motion. The proposed algorithm has resulted in a motion corrected result (as seen by the good agreement of the red ellipse marker with the inner boundary of the myocardium) which is reasonable for myocardial perfusion analysis. Next we show quantitative results on 9 dynamic perfusion exams acquired with a wide axial coverage (16 cm). Each exam consisted 15 cardiac volumes acquired at different time points with an average acquisition time of 35s. The end-end computational time of GPNLPerf was ≈ 6 *min* for processing a 4D dataset of dimensions $(512 \times 512 \times 224 \times 15)$, voxel size $(0.45 \times 0.45 \times 0.625)$, on a 8 core HP Z-800 workstation.

Here, for comparison, we choose ANTs [8] with a combination of Mutual Information [MI] and Local Cross Correlation [CC] as the metric posed in a

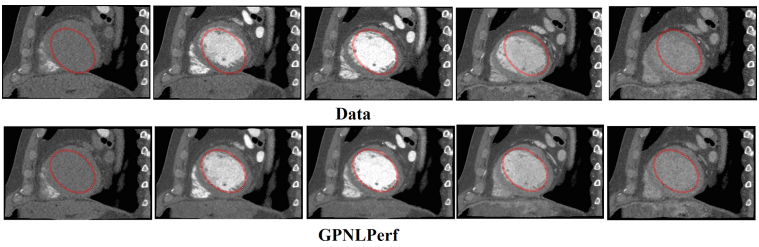

Fig. 4. GPNLPerf result on a 4D CT perfusion large motion case with 15 TPs. 5 TPs are shown in this figure. The alignment quality is visually seen in the red ellipse which lies very close to inner boundary of the myocardium post NRR.

symmetric diffeomorphic framework (SyN). Previous works in CT dynamic cardiac perfusion NRR ([2,3]) have mainly used MI and CC as registration metrics and posed in a reference based framework. Given that ANTs SyN has been quite successful in registration/segmentation competitions, we have used ANTs since it is similar in flavour to the above perfusion NRR works. The middle TP of each exam was picked as the reference volume for ANTs NRR. The pre-process steps and the deformation resolution (1.5 mm^3) are the same for GPNLPerf and ANTs. Below, we consider two validation metrics based on expert given LMs.

3.1 Spatial Alignment

To quantify motion correction achieved by NRR, an expert marked 4 different locations on the edge of the myocardium and at bifurcation points in most of the TPs of each exam. Each of the expert-marked landmarks formed a temporal cluster due to motion across TPs. To evaluate the efficacy of registration, distance of every landmark from its temporal cluster center is calculated. NRR should give improved temporal alignment resulting in lower distance values.

Figure 5 shows results after consolidating landmarks across datasets (9 exams, 4 landmarks, 294 landmarks in total), shows both ANTs and GPNLPerf reducing error compared to before registration. It can also be seen from the Scatter plot and error Histogram that GPNLPerf has resulted in *lesser, tighter* errors. It is also observed that the fine accuracy of GPNLPerf is better than ANTs resulting in a significant number of LMs having error $\leq 1.5\,mm$ (deformation field resolution) as seen from the histogram. A paired t-test between ANTs and GPNLPerf was done. The p-value was less than 0.001 and the 95 % confidence interval for the difference between ANTs and GPNLPerf results was 0.072 to 0.24 showing statistically significant improvement in alignment using GPNLPerf.

3.2 Intensity Trend Error

Another metric that we use to quantify registration accuracy is to compare intensity trends observed post NRR to Ground Truth [GT] trends. This metric would

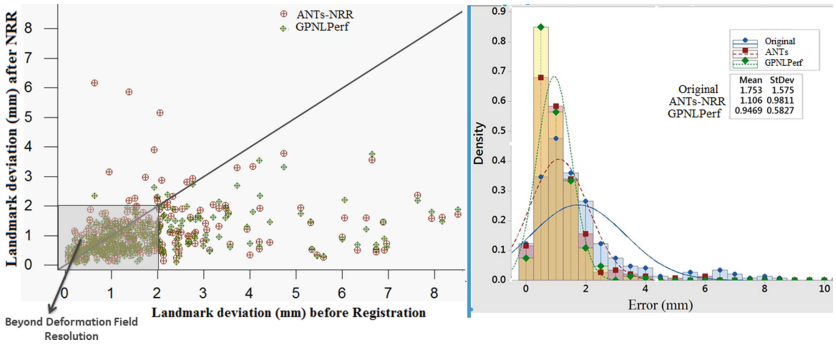

Fig. 5. Effect of registration at landmark locations (9 datasets: 4 landmarks, 294 landmarks in total). **Scatter Plot**: ANTs and GPNLPerf have brought about greater spatial coherence around landmark locations after registration. It can be seen that ANTs (red circles) has resulted in gross errors in a few cases. **Histogram**: a consolidated histogram of errors with a Gaussian fit for before NRR, ANTs, GPNLPerf errors is shown. GPNLPerf has resulted in lesser, tighter errors compared to ANTs.

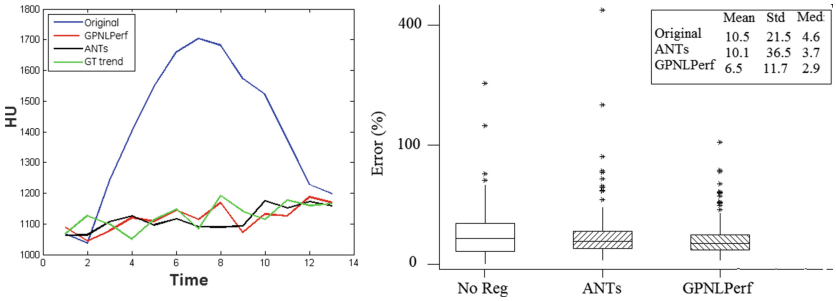

Fig. 6. Intensity trend compared to GT trend. For an example case, we see that the temporal intensity profile in the homogenous region closely matches the GT profile after registration (Left). The bar plot (on 9 cases, 15 TPs, 2 LMs) and statistics shows that GPNLPerf trend has matched well with the GT trend compared to ANTs.

additionally catch distortions introduced to the contrast dynamics. We evaluated the error between expert marked intensity profile (LM in homogeneous regions tracked by the expert over time) and profile post NRR at the LM location. On 9 datasets with two LMs each in the homogenous myocardium, the error with respect to the GT profile is seen to have reduced post NRR (Fig. 6, bar plot on the Right). GPNLPerf shows clearly better alignment ($\mu = 6.5, \sigma = 11.7$) (on 9 cases, 15 TPs, 2 LMs) with the GT intensity profile compared to ANTs.

3.3 Perfusion Maps

Here, we do a qualitative assessment of the resulting perfusion maps. The perfusion maps were derived using a deconvolution algorithm based on the

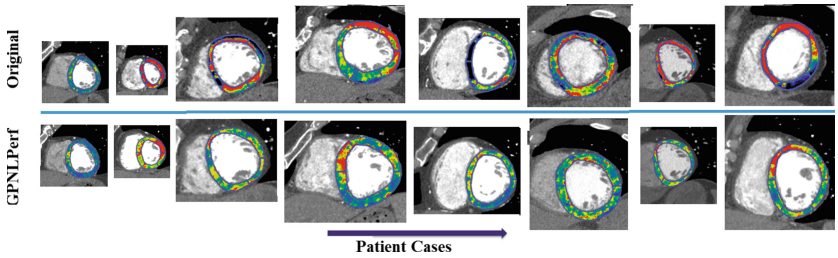

Fig. 7. Shown MBF computed before (Top row) and with GPNLPerf (Bottom row) for a few studies. MBFs after GPNLPerf seem more clinically relevant. (Color figure online)

Lawrence-Lee tissue model [9]. In Fig. 7, Myocardial blood flow (MBF) LUT of all screen captures have same color code (rainbow) and same threshold (0–250). GPNLPerf images show much better uniformity within the MBF whereas original images due to motion, show much wider values: very high values - red - due to cardiac cavity (both left and right ventricles) contamination and very low values - dark blue - because of pericardiac fat contamination. Thus, MBF estimations provided after GPNLPerf maps seem more clinically realistic and relevant.

4 Conclusion

In GPNLPerf, a fully automatic end-end solution for addressing the motion challenges of 4D CT perfusion studies is proposed. Quantitative landmark based comparison is done with ANTs and better NRR is demonstrated in terms of alignment and artifacts. Finally, the resulting perfusion maps are seen to be more clinically realistic after registration.

References

1. Varga-Szemes, A., Meinel, F.G., et al.: CT myocardial perfusion imaging. Am. J. Roentgenol. **204**, 487–497 (2015)
2. Fahmi, R., Eck, B.L., et al.: Dynamic CT myocardial perfusion imaging: detection of ischemia in a porcine model with FFR verification. In: Proceedings of SPIE (2014)
3. Isola, A.A., Schmitt, H., et al.: Image registration and perfusion imaging: application to dynamic circular cardiac CT. In: IEEE NSS/MIC 2010 (2010)
4. Kim, M., Wu, G., Shen, D.: Groupwise registration of breast DCE-MR images for accurate tumor measurement. In: ISBI (2011)
5. Mahapatra, D.: Joint segmentation and groupwise registration of cardiac perfusion images using temporal information. ISRN Mach. Vis. (2012)
6. Metz, C.T., Klein, S., et al.: Nonrigid registration of dynamic medical imaging data using nD+t B-splines. MIA **15**, 238–249 (2010)

7. Thiruvenkadam, S., Shriram, K., Manjeshwar, R., Wollenweber, S.: Robust PET motion correction using non-local spatio-temporal priors. In: Navab, N., Hornegger, J., Wells, W.M., Frangi, A.F. (eds.) MICCAI 2015. LNCS, vol. 9350, pp. 643–650. Springer, Heidelberg (2015). doi:10.1007/978-3-319-24571-3_77
8. Avants, B.B., Tustison, N.J., Song, G., Gee, J.C.: Ants: advanced open-source normalization tools for neuroanatomy. In: PICSL (2009)
9. Lawrence, K.S.S., Lee, T.Y.: An adiabatic approximation to the tissue homogeneity model for water exchange in the brain: a theoretical derivation. Nature **359**, 843–845 (1998)